Geochimica et Cosmochimica Acta Vol. 47, pp. 363–375

0016-7037/83/030363-13$03.00/0

Authigenic smectite on diatom frustules in Bolivian saline lakes

DENISE BADAUT
Institut de Géologie, 1 rue Blessig, 67084 Strasbourg, France

and

FRANÇOIS RISACHER
Mission ORSTOM, Cajon Postal 8714, La Paz, Bolivia

(*Received September* 2, 1981; *accepted in revised form November* 24, 1982)

Abstract—Observation under the electron microscope of diatom frustules from Bolivian Altiplano saline lakes shows that many of these are coated with particles occurring as tiny sheets. The frustules can be found to be almost completely replaced by these sheets. Isolated sheet aggregates seem to have resulted from completely transformed frustules. Section observations of altered frustules bear out that the sheets have grown from biogenic silica through replacement. Selected area diffraction, dark field observation, microdiffraction, and elemental microanalysis show that the particles on the diatom frustules consist of a poorly crystallized MG-smectite.

The unambiguous localisation of this authigenesis allows us to reconstruct its hydrochemical and sedimentological environment. Observation of the most recent lake sediments has pointed out that at least two main conditions are required for this authigenesis at 5°C: saturation with respect to amorphous silica, and a pH above 8.2. Variations in the Mg concentration have no significant effect.

INTRODUCTION

THE MAJOR mechanism of silica precipitation from natural waters (sea-water, fresh or salt water) is biochemical, essentially due to organisms such as diatoms, radiolaria, sponges, etc., which secrete a siliceous skeleton (SIEVER, 1957, 1962). The biochemical process of silica precipitation is an efficient one: the amount of biogenic opal formed in sea-water is estimated to 250×10^{14} gr. SiO_2 Y^{-1} by WOLLAST (1974). It is also a process which is not highly dependent on dissolved silica content: SIEVER (1962) sets the lower limit at 1 ppm, while the mean value in surface sea-water is 6 mg/l (GOLDBERG, 1957), and is 13.1 mg/l in river water (LIVINGSTONE, 1963). Biologically produced silica is amorphous and hydrated (Opal A, JONES and SEGNIT, 1971). Natural waters, including interstitial waters from superficial sediments, are highly undersaturated with respect to this opal. When protective cytoplasmic activity ceases, the biogenic silica usually redissolves (*cf.* behavior cycle of silica in oceanic environments: WOLLAST, 1974). Under certain conditions, however, in their natural medium, the siliceous skeletons show a certain resistance to dissolution, and can therefore accumulate:

—the majority of the silica to be found in ocean sediments is biological in origin. Mud containing diatoms and radiolaria is very widespread, and the cherts and porcelanites owe their existence to the diagenetic evolution of biogenic silica (LANCELOT, 1973; WEAVER and WISE, 1974; KASTNER, 1977).

—in continental environments, the existence of lacustrine diatomites testifies that the frustules have been preserved in the same manner.

When dealing with this particular problem, LEWIN (1961) showed experimentally that certain metal cations, and more especially Al and Fe (but not Ca and Mg) could be adsorbed onto diatom frustule walls, thereby slowing down the dissolution process. ILER (1979) pointed out that the diatom frustules have the same properties as silica gels:

—the specific area of the fresh frustules is greater than 100 m^2 g^{-1};

—these siliceous skeletons act as ion exchangers.

The capacity of silica gels to act in this way was studied from a theoretical standpoint by DUGGER *et al.* (1964). According to the results of this article, HURD (1973) stressed that the surface adsorption of various metal ions, such as Al^{3+}, Fe^{3+}, Mg^{2+}, Ca^{2+}, Cr^{3+}, UO_2^{2+}, etc. onto particles of biogenic silica is a quite plausible process in the pH and temperature conditions prevalent in superficial marine sediments. For DONNELLY and MERILL (1977), large quantities of magnesium are thus adsorbed onto the surface of the biogenic opal of marine sediments, VAN BENNEKOM and VAN DER MAREL (1976) suggested that the geochemical cycles of silicium and aluminium might be interconnected *via* diatom frustules.

The formation of a silicated layer on the surface of the biogenic opal can thus be seen to be widely considered as one of the first signs of interaction between biologic silica and the mineral world. For HURD (1973), VAN BENNEKOM and VAN DER MAREL (1976), DONNELLY and MERILL (1977), such a silicates layer would reduce dissolution rate of opal, depending on the conditions and the ion adsorbed, and also points to a possible authigenesis of clay on the surface of the biogenic silica particles. These au-

thors do not, however, afford any clear demonstration of such mineral development in natural conditions.

In two recent studies, BADAUT *et al.* (1979) and HOFFERT (1980) have referred to instances of authigenesis of smectites on diatom frustules. This paper gives a detailed description of the morphology, mineralogy and chemistry of thin sheets occurring in association with diatom frustules in Bolivian saline lakes.

GEOLOGIC SETTING

The Bolivian Altiplano is a wide Pliocene-Quaternary continental basin located between the Eastern and the Western Cordillera of the Andes (Fig. 1). This basin has been markedly affected by a strong acid volcanism (FERNANDEZ *et al.*, 1973), especially in the South Province of Lipez, where volcanoes are very close to each other, and delineate small, closed basins at high altitude (4,000 to 4,500 m).

The climate is characterized by a dry, cold winter (from March to November), and by a somewhat warmer and wet summer (from December to February). The lowest winter temperature may drop to −30°C. Rainfall averages 100 to 300 mm yearly, and the annual potential evaporation is about 1 to 1.5 m. Closed basins, where evaporation exceeds inflow, are the most favorable environments for saline lakes (EUGSTER and HARDIE, 1978). Slight climatic changes during the Quaternary period caused the level of the lakes to vary (SERVANT and FONTES, 1978). The present lakes and salars are the remnants of lakes which covered an area 6 times as large some 12,500 to 11,000 years ago. Desiccation of one of these ancient lakes in the center of the Altiplano has deposited the largest salt-pan in the world: the salar of Uyuni (ERICKSEN *et al.*, 1978; RETTIG *et al.*, 1980).

In the small intravolcanic southern basins, salt compositions vary from one basin to another, and range from sodium chloride, sodium sulfates, and sodium carbonates to calcium sulfates and borates (AHLFELD, 1956; AHLFELD and BRANISA, 1960; RISACHER, 1978). Sediments consist of diatom mud with calcite, gypsum, and clays. The samples studied in the first part of this paper are representative of the uppermost layers of the deposits, *i.e.* the still unconsolidated mud covering the bottom of the lowest sectors of approximately ten of these Lipez salars: Canapa, Hedionda, Chiar Khota, Honda, Pujio, Ramadita, Chulluncani, Pastos Grandes (Fig. 1).

STATEMENT OF THE PROBLEM

The clay found in the superficial lacustrine sediments was detected by X-ray powder diffraction analysis performed on the whole sample, but accurate identification by X-ray diffraction was problematic. The clay is present in small quantities only, and is mixed with other mineral phases, calcite, gypsum, salts, amorphous material; the treatment required for extraction seems to alter this clay. We shall see later that it is in fact a highly soluble microcrystalline magnesian smectite. It was virtually impossible to obtain characteristic diagrams of oriented less than 2 μ particles. The best diagrams, those of the smaller than 2 μ fraction of the deposits from the Canapa salars, show a rather distinctive smectite which does not really collapse at 10 Å after 4 hours at 490°.

In order to confirm the hypothesis concerning the origin of this clay, an attempt was made to characterize it more accurately. Whilst it may have been detrital in origin, according to RISACHER's hypothesis (1978) the volcanic environment and the evolution in the water chemistry were responsible for authigenesis by reworking of volcanic glass.

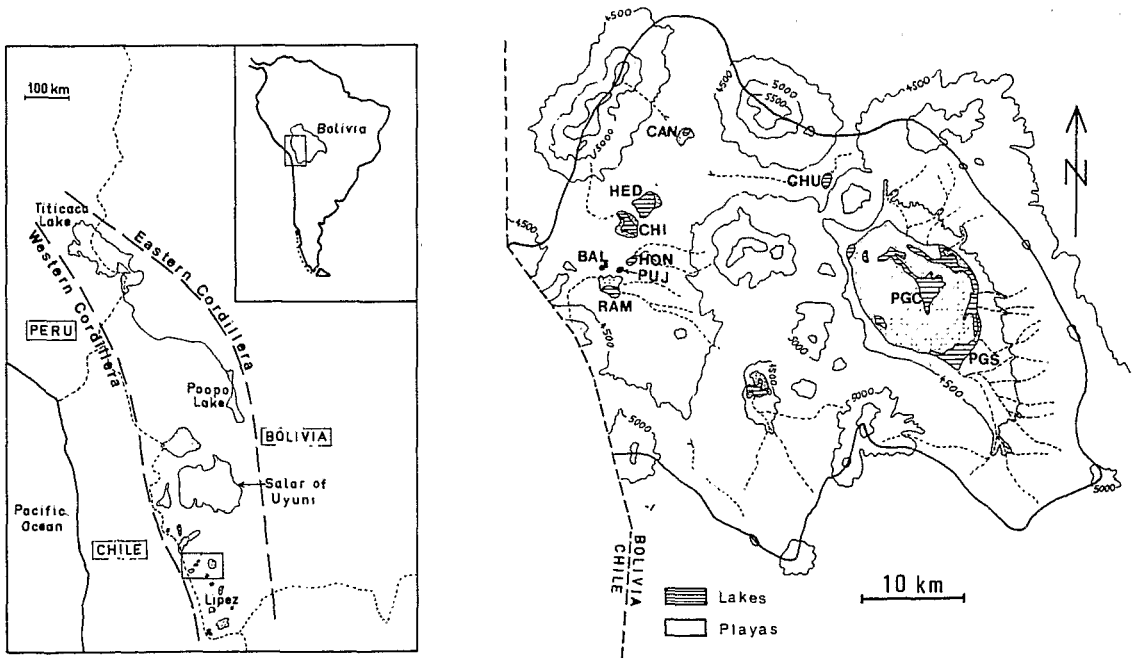

FIG. 1. Location maps. CHU: Chulluncani; CAN: Canapa; HED: Hedionda; CHI: Chiar Khota; HON: Honda; PUJ: Pujio; BAL: Ballivian; RAM: Ramaditas; PGC: Central Pastos Grandes; PGS: Southern Pastos Grandes. Unlabelled salar is a sodium carbonate lake.

New methods of investigation were therefore necessary, transmission electron microscope observation was adopted. This procedure revealed that the main constituents of these deposits, diatom frustule fragments, were sometimes coated with thin sheets. A further study of these sheets and their link with the biogenic silica required the use of the electron microscope techniques described below.

METHODS

Three types of microscope were used:

—A Philips EM_{300} transmission electron microscope, for observing particles, obtaining selected area diffraction diagrams and producing dark field images.

—A Cameca scanning microscope, fitted with an energy-dispersive spectrometer and a Tracor mini-computer for elemental analysis of isolated particles of the order of 1 μ.

—A JEOL 100CX scanning transmission electron microscope, for more accurate determination of the smallest crystallites (down to 100 Å).

The operation of a transmission electron microscope, and the obtaining of images and diffraction diagrams for selected areas (SAD pattern) have been described by several authors, such as HIRSCH *et al.* (1965) and MAGNAN (1961). We shall discuss only the dark field technique, which is as yet little used in the domain of earth sciences.

Principle

The diffraction pattern of crystalline materials takes shape in the back focal plane of the objective lens of the microscope; an aperture is set in this back focal plane, and is chosen small enough to allow only a given hkl beam to pass through; if, then, we form the optical image (in Gaussian plane), we obtain a bright image against a dark field. The regions of the object which appear bright on the dark field are those from which the selected (hkl) beam is given off. If the aperture does not intercept any beam, the optical image is entirely dark.

Application of dark-field electron microscopy to the study of disordered materials

The technique was adapted to study very small crystallized domains in a poorly crystallized material by OBERLIN *et al.* (1974, 1980). Indeed, if the ordered region is very small, the breadth of the scattered beam should be important, and it becomes undetectable in the diffraction pattern plane; in spite of this, the corresponding dark-field image remains bright and visible. Thus, in order to discover and investigate very small particles, the following procedure is adopted: a small aperture (generally less than 0.2 $Å^{-1}$ in the reciprocal space) is set in the back focal plane of the objective lens, and centered on the optical axis of the microscope. The optical image can then be observed (the projector lenses remain focussed on the Gaussian plane), while the incident beam is progressively tilted to explore radially the available reciprocal space; this is strictly equivalent to the displacement of the aperture in the Abbe plane and has the advantage of avoiding any spherical aberration effects. When the unscattered beam leaves the aperture, the image remains completely dark as long as no diffracted beam passes through the aperture. When crystallites light up, the aperture intercepts the hkl beam produced. The brightness reaches its maximum intensity when the aperture is exactly centered on the diffracted beam. A picture of the incident beam position relative to the aperture position is taken, which is superimposed on the SAD pattern of a suitable standard. The distance between the two images (incident beam, aperture) is measured, and the corresponding lattice-plane spacing can then be calculated. In addition, any hkl Debeye Scherrer ring can be explored by moving the incident beam along the perimeter of a circle. In conclusion, measurement of the lattice spacing is possible in this way, even when the diffracted beam itself is not visible on account of the small size of the crystalline region.

Overlapping or very thick particles cannot be studied by transmission electron microscopy (maximum thickness of a few hundred Å only). In order to circumvent this difficulty, the technique of inclusions and thin sections produced by ultramicrotomy used in biology (HAYAT, 1970) was adopted, with the modification suggested by EBERHART and TRIKI (1972,a,b), RAUTUREAU (1974). These sections are the subject of more detailed dark-field investigation.

Single particles were analyzed with an energy-dispersive spectrometer on a scanning electron microscope (SEM). Particles are first detected and localized with the transmission electron microscope (TEM), and thereafter the same preparation is studied with the SEM. When the TEM is not equipped with an X-ray spectrometer, this technique allows us to carry out elemental analysis of thin particles without any superimposition (checked by microdiffraction) nor any close interferences (checked by morphological observations). In order to obtain semi-quantitative results, the following formula was used:

$$E_i = \frac{k_i I_i}{\sum k_i I_i} \times 100$$

where E_i is the concentration in percent of element i, I_i is the peak area relative to the K_α ray of element i, and k_i is an empirical coefficient corresponding to the element i, determined by a previous calibration with sheet materials of known composition close to the studied mineral. Of course, in spite of the semi-quantitative nature of the determination, such a formula leads to perfectly balanced analyses. The largest errors result from the fact that we are unable to measure Na and Li. The Na K_α ray is overlapped by Cu L_γ ray of the grid-rack, and the technique does not apply to light elements such as Li. Finally, water does not appear in these results.

Physical aspects of electron probe analysis, and practical aspects of X-ray analysis of these samples in the scanning electron microscope, can be found in GOLDSTEIN and YAKOWITZ (1975) and MAURICE *et al.* (1978).

Scanning transmission electron microscopes enable elemental analysis to be carried out, and produce diffraction of electrons over areas down to 100 Å in diameter. These diagrams will henceforth be referred to as microdiffractions, in order to differentiate them from the SAD patterns obtained by classic electron microscopy (minimum diffraction area approximately 1 μ with an acceleration voltage of 100 Kev). The technical parameters involved in obtaining these results have been outlined in SUDO *et al.* (1981).

Thorough knowledge of clays in general was necessary in order to characterize the material studied. For electron microscopy, GARD (1971) was used as a basic guide, and articles by EBERHART and TRIKI (1972a,b) served more specifically as reference points for the analysis of section sheets.

RESULTS OF ELECTRON MICROSCOPE OBSERVATION

Morphology

Observation of sedimented particles under the transmission electron microscope reveals three types of diatom frustules: (1) whole, or broken but unaltered frustules characterized by homogeneous silica, clear fragment breaks and thin grids in the largest perforations of the tests—most of the whole frustules

are of this type; (2) corroded fragments with irregular breaks where the thin grids have disappeared; (3) fragments coated with tiny sheets (Plate I,1). Tiny sheets are more or less developed, and eventually the frustule fragment is completely replaced by them. The test framework can only be inferred from the whole sheet aggregate. Sometimes, the sheets seem to coat a corroded frustule. Independently of the transformed tests, clusters of tiny sheets (Plate I,2) are widespread throughout the whole preparation. All transitional morphology can be found between the sheet clusters and the completely replaced test fragments. However, this observation is not sufficient to prove that the sheet clusters result from completely transformed and torn-up frustule fragments.

Sections (about 500 Å thick) of sediment inclusions in a resin were observed in order to check the relationship between frustule silica and the tiny sheets. Plate I,3 shows a section of an unaltered frustule fragment. The biogenic silica fringes look quite clean. The scaly texture is an artefact due to the knife impact. At higher magnification, each scale looks homogeneous, without any visible micro-texture. Plate I,4 shows a section of a frustule whose fringe is wrapped by secondary material in which tiny elongated areas have developed. This material can extend to the whole particle, leaving only a reduced nucleus of biogenic silica (Plate II,1), which may completely vanish (Plate II,2). The clotted texture around the biogenic silica in Fig. 1, Plate II, is an artefact due to the high vacuum or to the beam (or both), upon the small elongated areas. Particles where biogenic silica is reduced or missing fairly often exhibit finely striated zones within, or more commonly on the periphery of, the tiny elongated areas (Plate II,2).

Ultra-sonic vibration of any intensity, with durations up to 30 min was unable to break up the bonds between biogenic silica and the sheets. On the other hand, long washing (20 to 30 hours in distilled water at room temperature) dissolved the sheets and left corroded frustules.

All these observations lead to the conclusion that a very strong bond exists between the sheets and the biogenic silica. The more silica decreases, the more the sheet formation increases, and seems to be ordered. Hence we have considered the possibility of a mineral authigenesis at the expense of the biogenic silica of diatoms.

Mineralogy

Selected area electron diffraction (SAD). Ring or point diagrams obtained from sedimented sheet clusters show that these sheets are crystalline (Plate I,2). Rings or points with hexagonal distributions are consistent with the hk reflections of a clay mineral whose interplanar spacing would be $d_{02} = 4.5$, $d_{20} = 2.6$ and $d_{06} = 1.53$. No 001 reflection could be obtained from the sheets in transverse sections.

Dark field observations. Electron microdiffraction of the different features (scales, elongated areas, striated zones) does not show any SAD pattern. The electron microscope dark-field technique was therefore adopted, as described above. In the dark field, biogenic silica behaves as an amorphous material of scale texture, and of medium, homogeneous and constant illumination.

A section through the thin sheet material is likely to be perpendicular to a large number of these sheets. The dark field images sought were therefore those relative to the most characteristic reflections of three-layer clay minerals in vertical section.

Very small objective apertures were used: 0.1 to 0.16 $Å^{-1}$ of apparent diameter in the plane of Abbe, corresponding respectively to 5 and 8 microns of real aperture.

As a first result, the crystallites of the sheet material bonded to silica frustules light up at the same time as those in the section of discrete sheet clusters. We may thus assume that these two features are made up of the same mineral.

The striated areas light up to a maximum as the objective aperture of 0.16 $Å^{-1}$ in the reciprocal plane is centered between 0.1 and 0.8 $Å^{-1}$ in this plane; an interplanar spacing of the reflective planes of 10 to 12 Å is inferred. Such data are consistent with the 001 reflection of a more or less dehydrated smectite whose sheets would be parallel to the incident beam.

The tiny elongated areas light up at the same time as the striated zones, and their illumination rises to a maximum when the 0.10 $Å^{-1}$ aperture is centered between 0.11 and 0.10 $Å^{-1}$ (Plate II,3). Then these areas are crystallized, and the interplanar spacing of the reflective planes ranges from 9 to 10 Å. Dark-field illumination for other positions of the 0.1 $Å^{-1}$ objective aperture on the 001 ring shows that several crystallite populations are obviously present, which emphasizes the highly disordered micro-crystalline texture. When the objective aperture is displaced to higher angles along the same radius, the crystallites light up more intensely again for 0.27 $Å^{-1}$ and 0.20 $Å^{-1}$, indicating d (hkl) equidistances of 4.75 Å and 3.60 Å respectively. Assuming that 4.75 is the second reflection order on the 001 lattice plane family, and 3.60 the third, the following interplanar spacing would be obtained: $d_{001} = 4.75 \times 2 = 9.50$ Å, and $d_{001} = 3.60 \times 3 = 10.8$ Å. These results correspond to the 001 interplanar spacing of a wholly dehydrated smectite. Nevertheless, they are not sufficient to decide definitely on the precise mineralogical nature of the crystallites.

Micro-diffraction. Using the narrow beam of a scanning transmission microscope, it was possible to obtain microdiffraction diagrams of the tiny sheets fringing the frustule fragments (Plate I,1). They correspond exactly to those of a standard clay (stevensite). Diagrams obtained from striated zones on microtome sections (see Plate I,4) show hk bands on both sides of the 001 reflection which are characteristic of a turbostratic order of smectite elemental sheets.

Conclusion. The tiny-sheet mineral developing from the biogenic silica is a three-layer clay of the smectite type.

Elemental analysis

Elemental analysis of single-sheet clusters. Sedimented sheet clusters were analysed with an energy-dispersive spectrometer on a SEM, as described above. Table 1 shows semi-quantitative analysis of sedimented particles. Samples 1 and 2, respectively a standard stevensite and a standard saponite recalculated on a water-free basis (sample TRAUTH, 1977), are included for comparison with SEM analysis. All these data suggest that the diatom frustules were replaced by an authigenic Mg-smectite. The excess of silica is likely to be due to the few relics of biogenic silica at the center of the particles as observed in microtome sections.

Elemental analysis of micro-areas down to 100 Å. A scanning transmission electron microscope enabled us to analyse the first sheets developed on the frustules, and to investigate the different materials of which the glomerules consisted.

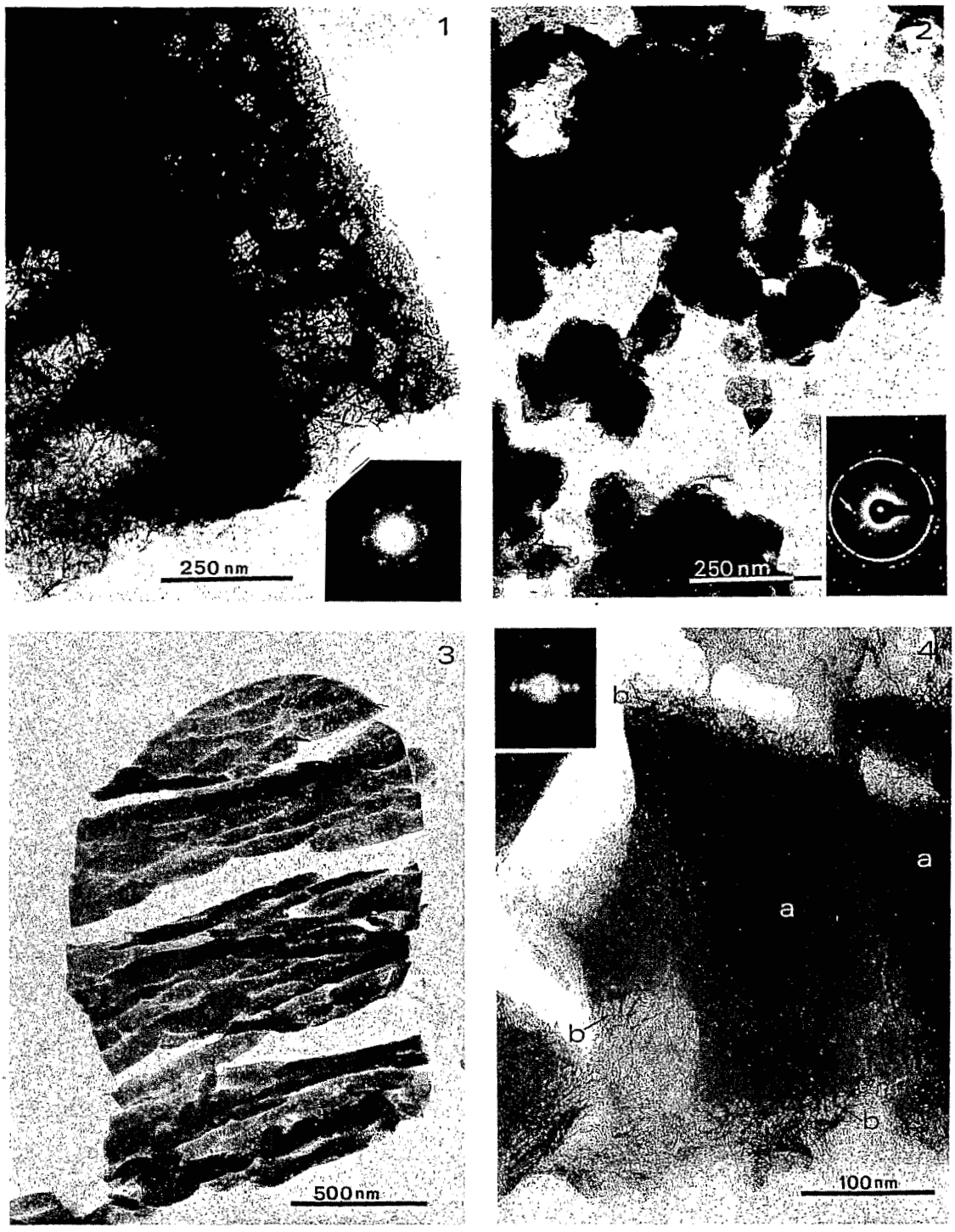

PLATE I,1. Frustule fragment coated with tiny sheets. Lower right inset shows a micro-diffraction diagram of sheets coating the perforations of the siliceous test (TEM photomicrograph).

PLATE I,2. Thin sheet aggregates. The lower right inset shows a SAD diagram of the thin sheets (marked by an arrow) and the gold internal standard (circles).

PLATE I,3. Section of an unaltered frustule fragment.

PLATE I,4. Silica chips (a) with elongated bodies (b) in a section of frustule fragment. The upper left inset shows a micro-diffraction diagram of the elongated bodies.

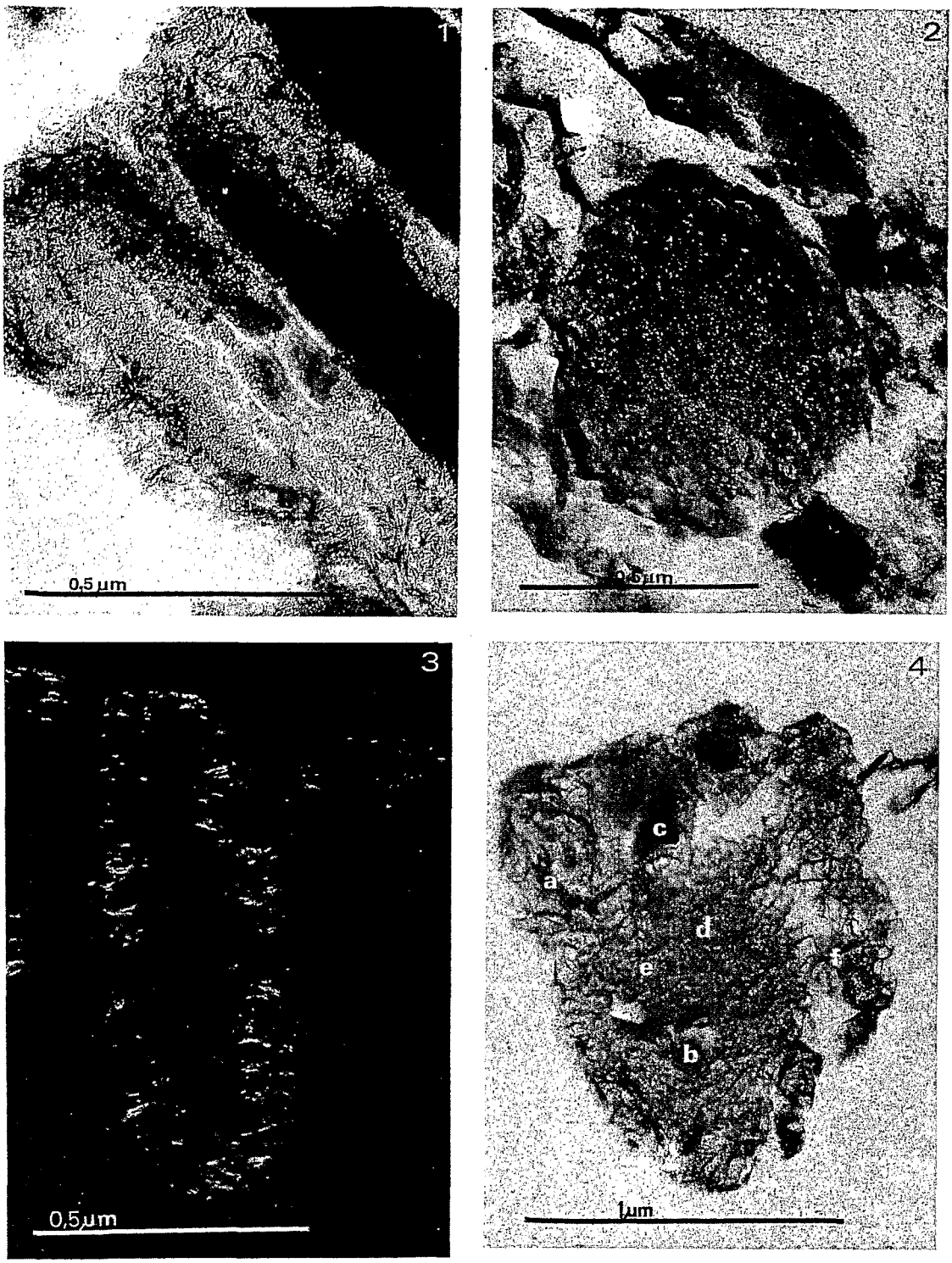

PLATE II,1. Section showing a biogenic silica relic in a sheet aggregate.

PLATE II,2. Section through a sheet aggregate. Silica is no longer observed whereas striped zones are present which are more visible in the granule margin.

PLATE II,3. Section through a frustule fragment coated with tiny sheets: 001 dark field image of three-layer clay mineral.

PLATE II,4. Section through an aggregate whose various parts: a to f have been analysed and reported in Table 2.

Table 1. Semi-quantitative elemental analysis of single sheet clusters (in %)
1 = standard stevensite ; 2 = standard saponite ; 3 to 7 are samples from Canapa Salar ; 8 and 9 are samples from Hedionda Salar.

	1	2	3	4	5	6	7	8	9
SiO_2	65.84	61.79	70.00	71.00	68.00	76.00	77.00	73.00	74.00
Al_2O_3	1.74	4.77	3.8	2.7	8.5	7.4	5.5	–	–
FeO	1.10	1.90	4.1	4.5	4.5	4.0	3.6	1.8	1.6
MgO	29.15	24.38	21.4	21.5	17.7	12.4	13.1	23.6	22.7
$CaO+K_2O$	0.45	1.42	0.7	0.3	1.3	0.2	0.8	1.6	1.7

The technique is based on counting the X-ray photons received by the spectrometer, and only enables quantitative comparisons with standard minerals to be made. Total count-rates for Fe, K and C were too weak to be used. Only Si, Mg and Al were detected in significant proportions. The results are given in Table 2. Samples 1 and 2 are the same stevensite and saponite samples as in Table 1. Analysis 3 confirms that the scale texture (in microtome section) is made of pure silica. Analyses 4 to 7 refer to tiny sheets on sedimented particles. Analyses 8 to 11 correspond to the authigenic material around the biogenic silica in section. Analyses (a) to (f) correspond to a thin section through a tiny sheet cluster, and are indicated on Plate II,4. They suggest some heterogeneity in the chemical composition of the clay fraction. The tiny elongated areas are deprived of Al, exactly as the tiny sheets on sedimented particles are (analyses 4 to 7), whereas the finely striated zones contain significant amounts of Al.

Conclusion of the electron microscope observation. It may be concluded that in the Bolivian Altiplano salars, biogenic silica takes a direct part in the formation of Mg-smectite nuclei. The growth of a clay mineral upon diatom frustules leads to sheet clusters of a Mg or Mg-Al smectite. The transformation of these frustules into clay will now be considered in its geochemical and sedimentological context, and an attempt will be made to identify the conditions necessary for this evolution to take place.

HYDROCHEMICAL AND SEDIMENTOLOGICAL ENVIRONMENT OF THE TRANSFORMATION

The transformation of diatom frustules enables two families of lakes to be distinguished. In five lakes (CAN, HON, PUJ, HED and CHU) authigenesis of clay takes place on the surface of the biogenic silica, at the expense of the latter. In the other five lakes (RAM, BAL, PGC, PGS and CHI), the frustules remain unaltered, or show only occasional very slight modifications (CHI). Almost all the salars are partly overlain by a shallow pool mostly fed by springs. In winter, water temperatures average 5°. The chemical composition of the brines does not strictly remain constant throughout the year. In summer, owing to rainfall, they may undergo some dilution for brief periods. Nevertheless, the lake levels remain stable for at least 9–10 months. It can be quite confidently assumed that no drastic change in the water chemistry has occurred since the present sediments were deposited. By careful analysis of this water chemistry, the conditions of clay authigenesis upon diatom frustules can be determined.

Hydrochemical environment

Analyses of lake waters are given in Table 3. Any Mg silicate precipitation may be schematically represented by the following reaction:

$$a\mathrm{Mg}^{++} + b\mathrm{H_4SiO_4} \rightarrow \text{Mg silicate} + 2a\mathrm{H}^{+}$$

High concentration in silica and magnesium as well as an increasing pH should increase the rate of such a reaction. The behavior of these components in the Bolivian saline lakes will therefore be examined.

Behavior of silica. The equilibrium reaction between silica and the aqueous solution can be expressed as follows:

$$\mathrm{SiO_2 \cdot} x\mathrm{H_2O} + (2-x)\mathrm{H_2O} \rightleftarrows \mathrm{H_4SiO_4}$$

$$a(\mathrm{H_4SiO_4})/a(\mathrm{H_2O})^{2-x} = K(T)$$

In brines, the activity of water, $a(H_2O)$, is no longer equal to 1, and it is therefore necessary to assign a value to x. In order to avoid such a choice, the following limiting values were considered: $x = 0$ (anhydrous silica), and $x = 2$ (total hydrated silica). The activity coefficient for H_4SiO_4 in a NaCl solution at 5°C (mean winter temperature) was extrapolated from MARSHALL's data (1980) for $NaNO_3$. Figure 2 plots the ionic activity product of silica *versus* total dissolved solids. All these waters are clearly saturated with respect to amorphous silica at 5°C.

Freshwater inputs already have a high silica content, *i.e.* 20 to 90 mg/l (RISACHER, 1978) due to the acid volcanic environment. As these waters evaporate and become saline, amorphous silica solubility decreases (MARSHALL and WARAKOMSKI, 1980). Low temperature also significantly decreases amorphous silica solubility (SIEVER, 1962; MAR-

Table 2 . Qualitative elemental micro-analysis of micro-areas down to 100 Å in diameter. The results are given with reference to a total of 1000 impulsions received by the spectrometer.

	1	2	3	4	5	6	7	8	9	10	11
Si	727	726	1000	717	730	724	733	749	735	750	740
Al	–	–	–	–	–	–	–	–	–	–	–
Mg	273	274	–	283	270	276	267	251	265	250	260

	a	b	c	d	e	f
Si	638	742	645	750	734	643
Al	213	–	151	–	–	146
Mg	149	258	204	250	266	211

TABLE 3. Chemical composition of lake waters in mg/l, except for alkalinity which is given in meq $(H^+)/m$. Waters a to f are Canapa interstitial brines

	Density	pH	ALK	Cl	SO_4	B	SiO_2	Na	K	Li	Ca	Mg
CAN	1.009	9.18	2.15	2 250	5 070	13	67	3 590	212	19.5	65	34
HON	1.015	8.05	4.40	10 300	2 600	57	68	6 740	990	47.0	200	140
RAM	1.020	8.15	2.93	13 900	3 070	77	89	7 600	1 030	11.8	1370	325
PUJ	1.022	8.85	7.22	14 500	4 320	145	56	10 000	1 020	37.0	400	210
BAL	1.032	8.18	4.88	22 000	5 700	150	54	13 500	1 700	25.5	1200	600
HED	1.050	8.50	10.00	24 600	18 500	235	59	19 800	2 100	122.0	520	650
CHI	1.051	8.28	8.05	38 500	4 080	250	74	20 700	2 500	176.0	1340	1140
CHU	1.087	8.80	35.00	44 000	26 600	960	47	30 100	12 800	22.5	730	1900
PGS	1.147	7.46	9.70	134 000	3 370	405	71	77 000	6 440	675.0	1650	1250
PGC	1.211	7.20	22.90	194 000	2 460	945	67	103 000	14 200	1640.0	3100	3480
a	1.136	7.52	7.55	109 000	18 800	495	69	69 000	8 020	519	862	1290
b	1.117	7.83	15.60	90 900	18 200	575	36	59 800	7 190	435	1030	1180
c	1.114	7.68	9.40	86 300	20 000	640	45	58 200	6 570	417	838	1160
d	1.108	7.64	10.00	80 900	22 500	615	42	55 200	6 140	389	702	1060
e	1.107	7.70	8.60	74 200	28 400	620	38	53 800	5 870	367	585	1030
f	1.114	7.79	13.40	74 900	34 200	570	43	56 600	6 330	380	573	1050

* Lake designation : CAN : CANAPA ; HON : HONDA ; RAM : RAMADITA ; PUJ : PUJIO ; BAL : BALLIVIAN ; HED : HEDIONDA ; CHI : CHIAR-KHOTA ; CHU : CHULLUNCANI ; PGS : PASTOS GRANDES-SOUTH ; PGC : PASTOS GRANDES-CENTER

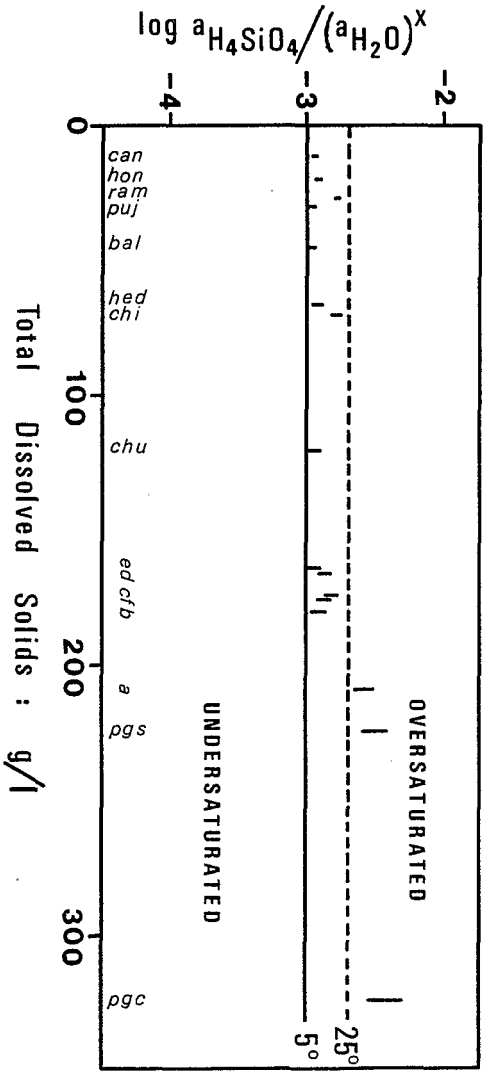

FIG. 2. Ionic activity product of amorphous silica: log $a(H_4SiO_4)/a(H_2O)^x$. Each water is plotted as a vertical segment whose ordinate is a function of x. (Lower and upper end correspond to $x = 0$ and $x = 2$, respectively).

SHALL, 1980). Silica saturation can therefore be reached, provided that diatoms are not able to control silica inputs.

Thus silica saturation in all of the lake waters cannot account for the difference between the two lake types.

Behavior of magnesium. Mg concentration ranges from 34 to 1900 mg/l for the lakes where diatoms are being transformed, and from 324 to 3480 mg/l for those where diatoms remain unaltered. Thus there is no relationship between Mg concentration and clay authigenesis in the Bolivian salars.

Behavior of pH. The five lakes where diatom frustules are rapidly transformed (CAN, HED, HON, PUJ, and CHU) all have pH ranging from 8.5 to 9.18, whereas the lakes where the frustules remain unaltered have lower values for pH, from 7.2 to 8.15, so high pH values are related to the neogenesis process.

Too little is known about the initial water (and the factors governing its evolution) to state clearly the reasons for this pH rise. However, the high pH values may be related to low Ca^{++} activity. If calcium activity decreases in these brines, carbonates are allowed to increase their own activity, and then the pH may rise.

The relationship between silica, magnesium and pH can be represented on a $MgO\text{-}SiO_2\text{-}H_2O$ activity diagram (Fig. 3). The authigenic Mg-smectite resembles stevensite. There are no data available on the stevensite stability field below 25°C. Since the chemical composition and natural occurrence of sepiolite are very close to those of stevensite, the activity diagram was constructed using the data at 0°C for sepiolite and amorphous silica from KHARAKA and BARNES (1973). The points representative of the five lakes where authigenesis take place are all located in the silica/sepiolite oversaturation area while the points relative to the other lakes are in the silica oversaturation area, or very close to it. On the other hand, this diagram shows why magnesium does not seem to be significant during the clay authigenesis: the square power of $a(H^+)$ is more important than $a(Mg^{++})$ in the expression: log $a(Mg^{++})/a(H^+)^2$.

Silica and magnesium are likely to be sufficient in all cases. Therefore the high pH values are related to the silica transformation and the neogenesis process.

So far we have studied the horizontal distribution of the authigenesis. Its vertical distribution in deeper

sediments will now be examined. For this purpose, the Canapa salar has been selected (CAN), where this process has been clearly detected as taking place in the mud of its superficial pool.

The sedimentological environment

Canapa is one of the smallest salars, with an area of about 1.25 km^2. Its basin was filled up with ancient lacustrine sediments. The surface of the playa is covered with a 1.3 cm thick mirabilite crust ($Na_2SO_4 \cdot 10H_2O$), except in the North, where a spring feeds a very shallow pool (20 cm deep). Very pure mirabilite is deposited within the upper sediments by capillary ascension up from a 2.3 m deep water table, and this forms local crusts up to 30 cm thick. On the whole, Canapa is a sodium chloride/sulfate salar.

Five sediment cores ranging from 80 to 150 cm in length were sampled in plastic pipes from the shore to the dry center of the playa. All the observations showed complete similarity between these five cores. Thus only the longest one is described in detail. Five interstitial brines were extracted on the field with a sediment squeezer (50 kg/cm^2). Another brine sample was collected from the water-table 3 m deep. Analysis of these waters appears in Table 3 (a to f).

Description of the longest core. Not enough sediments were available to perform precise sedimentological analysis. The only measurements taken therefore concern the height of the major peaks of powder and oriented pastes, X-ray diffraction diagrams adjusted by weighing the sediments before and after complete washing. Twelve samples were selected from the core. Figure 4 shows the mineralogical profiles. The mirabilite crust overlies to a gypsum bed which is continuous throughout the salar, and which is underlaid by a diatom-rich bed clearly lacustrine in origin. A downwards decrease in calcite is related to a small gypsum recurrence. The detrital smectite profile is based on the 14 Å peak intensities of the less than 2 μ perfectly washed sample fraction. Electron microscopy has revealed that the authigenic smectites are significantly dissolved after washing, whereas the detrital ones are preserved.

This profile thus shows the ratio between detrital smectites, and the other components of the less than 2 μ granulometric fraction especially biogenic silica. Halite and thenardite are partly dissolved in the interstitial brines.

The relative proportions of fresh (F), corroded (C) and clay pseudomorphs after diatom frustules (A) were estimated by approximate counting under the electron microscope (Fig. 4). In the upper gypsum bed, all of the frustules are replaced, whereas in the basal lacustrine sediments the transformation is much less advanced; unaltered frustules are as abundant as the replaced ones. Corroded frustules may often show the beginnings of transformation. The small gypsum recurrence in the lower part of the core can also be related to a stronger clay-authigenesis on the frustules.

Interpretation of the core profile. An ancient lake has deposited carbonate sediments. As it dried up, solutions followed the SO_4-rich/Ca-poor evaporation path. This is clearly marked by the end of the carbonate sedimentation, the gypsum bed and the superficial mirabilite crust. Diminution of detrital smectites reflects quite well the decrease in inputs from the drainage basin. In view of the good lateral continuity of the gypsum bed, it is very likely an original sedimentary deposit, and not a diagnostic precipitate. We

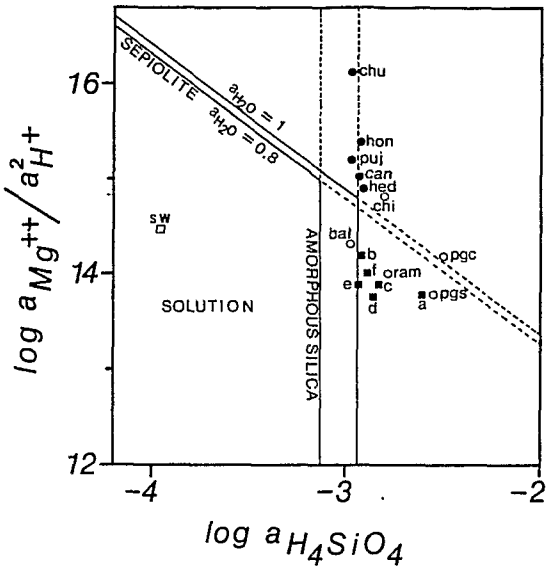

FIG. 3. MgO-SiO_2-H_2O activity diagram at 0°C. (Data from KHARAKA and BARNES, 1973). Dashed lines represent oversaturation for water activity of 0.8. Solid circles represent lake waters where diatoms are transformed. Open circles represent waters where diatoms remain unaltered. Squares are Canapa interstitial braines. SW = seawater. Water activities are ranging from 0.993 to 0.776.

can thus infer that during gypsum deposition, the pH may have increased to about 8.5–9.0. As silica was also likely to increase up to saturation concentration, both the conditions found in the present lakes where clay formation is rapid were fulfilled during the drying up of the ancient lake Canapa.

Each diagram (Figs. 2, 3) includes the representative points of the interstitial brine chemistry. They appear to be more closely associated with waters where no rapid clay formation occurs. It is nevertheless possible that the smectites are growing or reorganizing slowly. The Mg concentration factor in the interstitial brines is 1.25, *i.e.* less than for chloride (1.47).

DISCUSSION

It would be helpful to make a brief comparison with experimentally synthesized three-layer magnesian clays on the one hand, and with natural authigenesis previously investigated on the other, whether they be recent or not.

Experimental synthesis of three-layer magnesian clay

At normal temperature and pressure, three-layer clays with magnesian octahedra are the easiest to synthesize. Experiments conducted on solutions or gels have shown that the conditions required for neoformation of three-layer magnesian clays consist essentially of saturation with respect to amorphous silica, and an elevated pH. SIFFERT (1962) succeeded in synthesizing a smectite-type magnesian clay 20°C using dilute solutions (0.3 g/L $MgCl_2$) with a pH

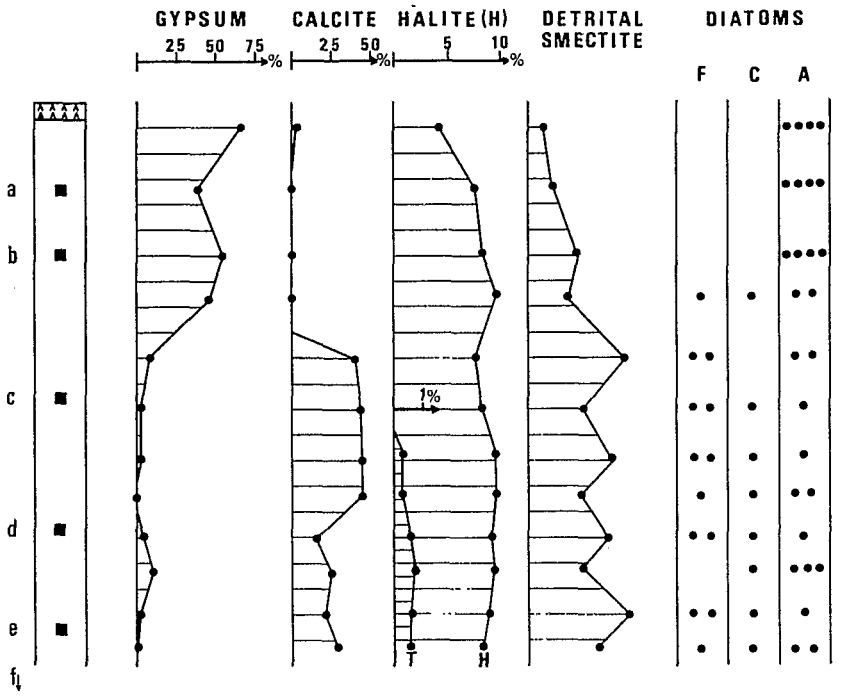

FIG. 4. Canapa Salar. Sedimentological profiles of the main core. Total core length: 1–5 m. Squares correspond to interstitial water samples. Water f was sampled 1.5 m below water e. Percentages are semi-quantitative. In the halite profile: H = halite, T = thenardite. In the diatom profile, F = fresh, C = corroded, A = argillization (*i.e.*, clay authigenesis). Each solid circle represents roughly 25% of the total diatom content.

value greater than 10, but saturated with respect to amorphous silica. He even remarked that crystallization of the resultant product was enhanced when the quantity of Mg in contact with the silica was reduced. WOLLAST *et al.* (1968) precipitated another magnesian clay mineral, sepiolite, by adding silica to seawater, with pH adjusted to 8. They also showed that when the pH value is reduced to 7, even in silica-saturated seawater, no sepiolite is produced. More recently, DECARREAU (1980) has mastered the synthesis of magnesian smectites—stevensite and hectorite—from silico-magnesian co-precipitates. He also pointed out that the aqueous phase, in equilibrium with the forming material, was characterized by silica saturation with low concentration of magnesium and a pH value of approximately 10. As in Siffert's experiments, excess magnesium slowed down the crystallogenesis, without modifying the process radically, and that synthesis of magnesian smectites took place just as readily in the presence or absence of electrolyte (NaCl, SO_4Na, $CaCl_2$).

These experiments confirm the fact that there is no direct link between the authigenesis of TOT magnesian phyllites and the salinity of the water, and more especially the magnesium content of the water. Even when this Mg concentration is low, rapid precipitation of TOT magnesian clays depends directly on the concentration of OH^- ions in the solution when the dissolved silica reaches saturation point. In continental environments, this silica concentration often occurs through evaporation, which explains why naturally occurring magnesian smectites are often linked to saline environments.

With reference to the high pH apparently necessary for these authigeneses to take place, as SIFFERT (1962) pointed out, high magnesium concentrations can occur in solutions which are sufficiently basic for the silicic acid (H_4SiO_4) to be partly dissociated ($H_3SiO_4^-$, $H_2SiO_4^=$); in this case, the silanol groups are immediately available for synthesizing reactions. This remark appears especially interesting in the context of the Bolivian salars, where authigenic clay minerals develop on the surface of the diatom frustules. The images studied show that the whole siliceous surface is covered by a dense, uninterrupted layer of clay nuclei. This can easily be explained by the density of the silanol groups on the surface of biogenic silica (up to 4 per nm^2 according to YARIV and GROSS (1979) and LABEYRIE (1979). The solubility of other ions, such as Al and Fe is different from that of Mg (precipitation of Ferrous Hydroxide ($Fe(OH)_2$ when pH is greater than 6, covalency 4 of aluminum when pH value is high . . .), and it is therefore probable that authigenesis of Fe smectite or Al smectite from biogenic silica will adopt different forms, perhaps more closely connected to micro-en-

vironments, with respect to the H^+ delocalisation ("cauliflower"-type growth of clay at certain points on the surface, or in skeletal perforations).

Authigenic clay minerals in the Bolivian salars can only develop by magnesium uptake in the solution. The silica present in the solution may well contribute to crystallite growth. Since silicium is a relatively scarce element in solution, any reduction in the number of ($H_3SiO_4^-$) ions or siliceous molecules will give rise to a localized deficit, a local desaturation with respect to amorphous silica which will encourage opening of the neighbouring $\begin{matrix}\diagdown & \diagup \\ -SiOSi- \\ \diagup & \diagdown\end{matrix}$ bonds; this could explain the progression of the clay formation at the expense of the biogenic silica.

Natural authigenesis of magnesian smectites

Ancient authigenesis. On the basis of geological arguments (stratigraphy, mineralogy, etc.), MILLOT (1964) suggested that the sepiolites and smectites belonging to the ancient series of carbonates, clays and gypsum could be authigenic. He reconstructed the environment and described their formation in "chemical alkaline sedimentary basins". Later research confirmed this view. HUERTAS (1970) stressed the place of stevensite in basic sedimentation. TRAUTH (1977) refers to evaporites when dealing with sepiolites and stevensites of the continental and epicontinental series.

Modern authigeneses. Examples of modern continental authigeneses enable us to have direct access to the conditions governing this authigenesis but they are unfortunately quite rare occurrences. Apart from the Bolivian lakes, the only known occurrences are those discovered in the Chad basin. TARDY *et al.* (1974) and CHEVERRY (1974) describe the development of magnesian smectites in the interdune depressions to the north of the lake when evaporation produces a silica concentration and a rise in the pH (sodic carbonate environment; AL DROUBI, 1976). CARMOUZE (1976) describes a similar authigenesis in the interstitial waters of the northern part of the lake itself. By experimental evaporation of the water running into the lake (taken from the river Chary), free of any suspended matter, GAC *et al.* (1977) and GAC (1980) obtained a product very similar to the magnesian smectites synthesized by DECARREAU (1980), on condition that the silica concentration was at least 68.8 mg/l with a pH value of 9.5 and a magnesium concentration of 7.9 mg/l. GAC pointed out, however, that the presence of clay in suspension brought on premature fixation of Mg and Si in the silicoaluminous structures, thereby precluding formation of magnesian smectite at a later stage.

In the Lipez salars, detrital contribution was observed to cease at the same time as authigenesis of magnesian smectite began to take place, although it was not possible to state that this is a necessary condition.

In none of these instances of natural authigenesis of magnesian smectites has the role played by diatoms been mentioned, although these algae are ubiquitous and known to have existed since the Mesozoic era. They develop in lake Chad, for instance, where SERVANT-VILDARY (1978) has studied them systematically. In the Bolivian salars, the geochemical conditions are suitable for the authigenesis of magnesian smectites, although this only takes place on the surface of the frustules. One may legitimately ask whether it may not often be precisely this siliceous surface which, in natural conditions, induces and fosters the authigenesis process.

Authigenesis in oceanic environments. The requisite conditions for authigenesis, as seen above—large quantities of biogenic silica particles, elevated pH values, concentrated dissolved silica—are indeed the conditions which led HURD (1973), DONNELLY and MERILL (1976), WOLLAST (1974) and DREVER (1974, p. 348) to state that siliceous deposits in the oceans favour the authigenesis of magnesian clay minerals (sepiolites and attapulgites); in other sediments, the ability of the magnesium and silica to be incorporated into other pre-existing mineral phases, especially detrital clays (DREVER, 1974), would prevent this authigenesis from being instigated.

Figure 3 plots the average composition of a seawater sample. The dissolution of particles of biogenic silica or volcanic glass, increases the silica concentration in this water from marine deposits; after the first 20 cm of sediment, the water contains 5 to 10 times the concentration of silica to be found in the seawater itself (GIESKES, 1975; HURD, 1973; SCHINK *et al.*, 1974). The reasons for the rise in pH are more difficult to identify. ANDREWS (1977) and SEYFRIED *et al.* (1978) speculated on a possible pH rise during seawater-basalt interaction at low temperature. For WOLLAST *et al.* (1968) photosynthetic activity causes a rise in the seawater pH, but only at a shallow level of photosynthetic activity. It is possible that some dissolution of carbonate, especially skeleton organisms, is taking place (KASTNER, 1977).

CONCLUSIONS

The evolution of biogenic silica from the moment it is integrated into the sedimentary cycle is especially interesting, as it often represents both the least stable mineral phase of superficial deposits and a potential source of silica. CHAMLEY and MILLOT (1972) and HOFFERT (1980) have demonstrated that dissolution of diatom frustules can act as a "remote feeder" for smectite authigenesis. In the early stages of diagenesis the evolution of the biogenic opal (dissolution, transformation, persistence), is undeniably conditioned by geochemical factors such as the chemistry of the solutions and the mineralogical environment within the

deposit. KASTNER (1977) gives experimental proof of the influence of geochemical factors on the transformation of the biogenic opal into CT opal or quartz. LANCELOT (1976) observes the influence of the composition of the host-sediment on the same evolutionary process (A opal → CT opal or quartz).

In the Lipez Salars, when the water pH is high and the concentration of dissolved silica is close to saturation with respect to amorphous silica, biogenic silica has been shown to play a direct role in the authigenesis of magnesian smectite; in those waters which are saturated in silica, but with a lower pH value, the frustules remain unaltered. The magnesian nuclei which develop on the surface of the biogenic silica do not protect it from dissolution. Crystalline growth takes place progressively at the expense of the silica itself, and quickly conceals it; ultimately, the biogenic silica disappears totally, to make way for clay: the ephemeral nature of the process may explain why this mineral paragenesis was not identified earlier.

REFERENCES

AHLFELD F. (1956) Sodaseen in Lipez (Bolivien). *Neues Jb. Miner. Mh.* **6/7**, 128–136.

AHLFELD F. and BRANISA L. (1960) *Geologia de Bolivia.* Instituto Boliviano Petrolero, La Paz, 245 p.

AL DROUBI A. (1976) Geochimie des sels et des solutions concentrées par évaporation. Modèle thermodynamique de simulation. Application aux sols salés du Tchad. *Sci. Géol., Mém.* **46**, 177 p.

ANDREWS A. J. (1977) Low temperature fluid alteration of oceanic layer 2 basalts, D.S.D.P. Leg 37. *Can. J. Earth. Sci.* **14**, 911–926.

BADAUT D., RISACHER F., PAQUET H., EBERHART J. P. and WEBER F. (1979) Néoformation de minéraux argileux à partir de frustules de Diatomées: le cas des lacs de l'Altiplano bolivien. *C.R. Acad. Sci. Paris* **289**, D, 1191–1193.

CARMOUZE J. P. (1976) La régulation hydro-géochimique du lac Tchad. *Travaux et Documents de l'ORSTOM* **58**, 421 p.

CHAMLEY H. and MILLOT G. (1972) Néoformation de montmorillonite à partir de diatomées et de cendres dans la sédiments marins de Santorin (Méditerranée occidentale). *C.R. Acad. Sci. Paris* **274**, D, 1132–1134.

CHEVERRY C. (1974) Contribution à l'étude pédologique des polders du lac Tchad. Dynamique des sels en milieu continental sub-aride dans des sédiments argileux et organiques. Thèse Fac. Sci. Strasbourg, 275 p.

DECARREAU A. (1980) Cristallogenèse expérimentale des smectites magnésiennes: hectorite, stévensite. *Bull. Minér.* **103**, 579–590.

DREVER J. I. (1974) The magnesium problem. In *The Sea* (ed. E. D. Goldberg) Vol. 5, pp. 337–357. Interscience.

DONNELLY T. W. and MERRILL L. (1977) The scavenging of magnesium and other chemical species by biogenic opal in deep sea sediments. *Chem. Geol.* **19**, 167–186.

DUGGER D. L., STANTON J. H., IRBY B. N., MCCONNEL B. L., CUMMINGS W. W. and HAATHAN R. W. (1964) The exchange of twenty metal ions with the weakly acidic silanol group of silica gel. *J. Phys. Chem.* **68**, 756–760.

EBERHART J. P. and TRICKI R. (1972a) Description d'une technique permettant d'obtenir des coupes minces de minéraux argileux par ultramicrotomie. Application à l'étude des minéraux interstratifiés. *J. Microscopie* **15**, 111–120.

EBERHART J. P. and TRICKI R. (1972b) Essai d'identification de minéraux argileux par microdiffraction électronique en utilisant la réflexion basale 001. *Bull. Gr. Fr. Argiles* **24**, 3–14.

ERICKSEN G. E., VINE J. D. and BALLON R. (1978) Chemical composition and distribution of lithium-rich brines in Salar de Uyuni and nearly salars in Southwestern Bolivia. *Energy* **3**, 355–363.

EUGSTER H. P. and HARDIE L. A. (1978) Saline lakes. In *Lakes: Chemistry, Geology, Physics* (ed. A. Lerman), pp. 237–293. Springer-Verlag.

FERNANDEZ A., HORMAN P. G., KUSSMAUL S., MEAVE J., PICHLER H. and SUBIETA T. (1973) First petrologic data on young volcanic rocks of SW-Bolivia. *Tschermaks Min. Petr. Mitt.* **19**, 149–172.

FRITZ B. (1981) Etude thermodynamique et modélisation des réactions hydrothermales et diagénétiques. *Sci. Geol., Mém.* **65**, 203 p.

GAC J. Y. (1980) Géochimie du bassin du lac Tchad. *Travaux et Documents de l'ORSTOM* **123**, 251 p.

GAC J. Y., AL DROUBI A., FRITZ B. and TARDY Y. (1977) Geochemical behaviour of silica and magnesium during the evaporation of waters in Chad. *Chem. Geol.* **19**, 3, 187–215.

GARD J. A. (1971) The electron optical investigation of clays. *Miner. Soc. Monogr.* **3**, London, 381 p.

GIESKES J. M. (1975) Chemistry of interstitial waters of marine sediments. *Am. Rev. Earth. Planet. Sci.* **3**, 433–453.

GOLDBERG E. D. (1957) Biogeochemistry of trace metals. In Treatise on Marine Ecology and Paleoecology. Vol. 1, Ecology (ed. J. W. Hedgpeth) *Geol. Soc. Amer. Mem.* **67**, 345–357.

GOLDSTEIN J. I. and YAKOWITZ M. (1975) *Practical Scanning Electron Microscopy. Electron and Ion Microprobe analysis.* Plenum Press, 582 p.

HAYAT M. A. (1970) *Principles and techniques of electron microscopy. Biological applications*, I, Van Nostrand-Reinhold, London.

HEGELSON H. C. (1969) Thermodynamics of hydrothermal system at elevated temperatures and pressures. *Amer. J. Sci.* **267**, 729–804.

HIRSCH P. B., HOWIE A., NICHOLSON R. B., PASHLEY D. W. and WHELAN M. S. (1965) *Electron Microscopy of Thin Crystals.* Butterworths, N.Y., 549 p.

HOFFERT M. (1980) Les "argiles rouges des grands fonds" dans le Pacifique Centre-Est. Authigenèse, transport, diagenèse. *Sci. Géol. Mém.* **61**, 331.

HUERTAS F., LINARES J. and MARTIN-VIVALDI J. L. (1970) Clay minerals geochemistry in basic sedimentary environments. Reunion hispano-belga de minerales de la arcilla. (ed. J. M. Serratosa), C.S.I.C., Madrid, 211–214.

HURD D. C. (1973) Interactions of biogenic opal, sediment and seawater in the Central Equatorial Pacific. *Geochim. Cosmochim. Acta* **37**, 2257–2282.

ILER R. W. (1979) *The Chemistry of Silica.* Wiley, Interscience, London, 866 p.

INGRI N. (1963) Equilibrium studies of polyanions containing B^{III}, Si^{IV}, Ge^{IV} and V^{V}. *Svensk Kemisk Tictskrift* **75**, 4, 199–230.

JONES J. B. and SEGNIT E. R. (1971) The nature of opal. I—Nomenclature and constituent phases. *J. Geol. Soc. Australia* **18**, 56–68.

KASTNER M., KEENE J. B. and GIESKES J. M. (1977) Diagenesis of siliceous oozes. I. Chemical controls on the rate of opal A to opal CT transformation—an experimental study. *Geochim. Cosmochim. Acta* **41**, 1041–1059.

KHARAKA Y. K. and BARNES I. (1973) SOLMNEQ: solution-mineral equilibrium computation. USGS-WRD-73-002.

LABEYRIE L. (1979) La composition isotopique de l'oxygène de la silice des valves diatomées. Mise au point d'une nouvelle méthode de paléoclimatologie quantitative. Thèse Sci., Orsay, 171 p.

LANCELOT Y. (1973) Chert and silica diagenesis in sediments from the central Pacific. In *Initial Reports of the Deep Sea Drilling Project.* (eds. E. L. Winterer, J. I. Ewing *et al.*) vol. XVII, 377–405.

LANCELOT Y. (1976) Evolution geodynamique et histoire sédimentaire de deux grands bassins océaniques. (Atlantique NW et Pacifique). Thèse Sci., Paris, 301 p.

LEWIN J. C. (1961) The dissolution of silica from diatom walls. *Geochim. Cosmochim. Acta* **21,** 182–198.

LIVINGSTONE D. A. (1963) Chemical composition of rivers and lakes. *U.S. Geol. Surv. Prof. Paper 440-G,* 64 p.

MAGNAN C. (1961) *Traité de microscopie électronique.* Herman, Paris.

MARSHALL W. L. (1980) Amorphous silica solubilities. III—Activity coefficient relations and predictions of solubility behavior in salt solutions, 0–350°C. *Geochim. Cosmochim. Acta* **44,** 925–931.

MARSHALL W. L. and WARAKOMSKI J. M. (1980) Amorphous silica solubilities. II—Effect of aqueous salt solutions at 25°C. *Geochim. Cosmochim. Acta* **44,** 915–924.

MAURICE F., MENY L. and TIXIER R. (1978) *Microanalyse et microscopie électronique à balayage.* Les éditions de physique. Orsay, 534 p.

MILLOT, G. (1964) *Géologie des Argiles.* Masson et Cie Paris, 499 p.

OBERLIN A., BOULMIER J. L. and DURAND B. (1974) Electron microscope investigation of the structure of naturally and artificially metamorphosed kerogens. *Geochim. Cosmochim. Acta* **38,** 647–650.

OBERLIN A., BOULMIER J. L. and WILLEY M. (1980) Electron microscopic study of kerogen microtexture. Selected criteria for determination of kerogen evolution path and evolution stage. In *Kerogen* (ed. B. Durand) pp. 191–241. Technip, Paris.

RAUTUREAU M. (1974) Analyse structurale de la sépiolite par microscopie électronique. Relation avec les propriétés physico-chimiques. Thèse Sci. Orléans, 89 p.

RETTIG S. L., JONES B. F. and RISACHER F. (1980) Chemical evolution of brines in the Salar of Uyuni, Bolivia. *Chem. Geol.* **30,** 57–79.

RISACHER F. (1978) Le cadre géochimique des bassins à évaporites des Andes boliviennes. *Cah. ORSTOM,* sér. Géol. **10,** 37–48.

SCHINK D. R., FANNING K. A. and PILSON M. E. Q. (1974) Dissolved silica in the upper pore waters of the Atlantic Ocean floor. *J. Geophys. Res.* **79,** 2243–2250.

SERVANT M. and FONTES J. CH. (1978) Les lacs quaternaires des hauts plateaux des Andes boliviennes. Premières interprétations paléoclimatiques. *Cah. ORSTOM,* sér. Géol. **10,** 9–23.

SERVANT-VILDARY S. (1978) Etude des diatomées et paléolimnologie du bassin tchadien au cénozoïque supérieur. *Trav. et Doc. ORSTOM* **84,** 346 p.

SEYFRIED W. E. JR., SHANKS W. C. III and DIBBLE W. E. JR. (1978) Clay mineral formation in D.S.D.P. Leg 34 basalt. *Earth Planet. Sci. Lett.* **41,** 265–275.

SIEVER R. (1957) The silica budget in the sedimentary cycle. *Amer. Mineral.* **42,** 821–841.

SIEVER R. (1962) Silica solubility, 0–200°C and the diagenesis of siliceous sediments. *J. Geol.* **70,** 127–150.

SIFFERT B. (1962) Quelques réactions de la silice en solution: la formation des argiles. *Mém. Serv. Carte Géol. Als. Lorr.* **21,** 86 p.

SUDO T., SHIMODA S., YOTSUMOTO H. and AITA S. (1981) *Electron Micrographs of Clay Minerals.* Developments in Sedimentology, **31,** Elsevier, Amsterdam.

TARDY Y., CHEVERRY C. and FRITZ B. (1974) Néoformation d'une argile magnésienne dans les dépressions interdunaires du lac Tchad. Application aux domaines de stabilité des phyllosilicates alumineux, magnésiens et ferrifères. *C.R. Acad. Sci. Paris* **278,** D, 1999–2002.

TRAUTH N. (1977) Argiles évaporitiques dans la sédimentation carbonatée continentale et épicontinentale tertiaire. *Sci. Géol., Mém.* **49,** 195 p.

VAN BENNEKOM A. J. and VAN DER GAAST S. J. (1976) Possible clay structures in frustules of living diatoms. *Geochim. Cosmochim. Acta* **40,** 1149–1152.

WEAVER F. M. and WISE S. W. (1974) Opaline sediments of the southeastern coastal plain and Horizon A: biogenic origin. *Science* **184,** 899–901.

WOLLAST R. (1974) The Silica Problem. In *The Sea* (ed. E. D. Goldberg), Vol. 5, pp. 359–425. Interscience.

WOLLAST R., MACKENZIE F. T. and BRICKER O. P. (1968) Experimental precipitation and genesis of sepiolite at earth-surface conditions. *Amer. Mineral.* **53,** 1645–1662.

YARIV S. and GROSS H. (1979) *Geochemistry of Colloïd Systems.* Springer Verlag, Berlin, 450 p.

APPENDIX

Molal activities were computed with the aid of a microcomputer APPLE II PLUS 48 K. The program takes the temperature effect into account. Thermodynamic constants $K(T)$ are mostly those from the program EQUIL (FRITZ, 1981 and pers. commun.) computed from HELGESON (1969) and KHARAKA and BARNES (1973). Formation of borate polyanions (INGRI, 1963) prevents the distinction between carbonate and borate alkalinity above roughly 50 mg/l B. Therefore saturation with respect to calcite cannot be tested confidently. Otherwise, results are not much disturbed by boron.